Revista de Chimie
https://revistadechimie.ro
https://doi.org/10.37358/Rev.Chim.1949

Direct Hydrogenation and Hydrotreating of Neat Vegetal Oil into Renewable Diesel Using Alumina Binder with Zeolite

SHANMUGAM PALANISAMY*, KANNAN KANDASAMY
School of Chemical and Food Science, Kongu Engineering College, Erode-638 060, India

Abstract: *Hydrodeoxygenation of vegetal oil and methyl oleate studied using Pt and Pd supported with alumina-beta-zeolite (γ-Al_2O_3-H-β) and comparing its performance with NiMo/γ-Al_2O_3 and Pd/C in a semi-batch reactor, at 300 - 340 °C and 2.0 MPa. This study has used Pd and Pt on H-β zeolites with alumina binder as extrudate and it examines over triglycerides hydrogenolysis. Pd/C showed higher rate of deoxygenation and the selectivity of C_{18}/C_{17} was higher for NiMo-S/γ-Al_2O_3 and PdPt/γ-Al_2O_3-H-β. PdPt/γ-Al_2O_3-H-β enhanced the hydrogenation and hydrogenolysis, while conversion and yield in deoxygenation and decomposition has reached identicical performance as NiMo-S/γ-Al_2O_3 catalytic deoxygenation process. Both the thermal decomposition and the hydrogenation of unsaturated triglycerides were mainly affected by H_2 partial pressure. Transition metals like Pd and Pt on H-β and alumina binder ratio of 40:60 wt% showed effective hydrodeoxygenation of vegetal oil without substituting sulfur feed.*

Keywords*: Hydroprocessing, Vegetal oil, Alumina, Carbon, Zeolite*

1. Introduction

In the present scenario, few refineries are involved in producing biomass based diesel-like fuel, named as renewable diesel, to replace the conventional one [1-5]. In the last two decades, raw vegetal oils, animal fats and algal oils had been converted into renewable diesel by catalytic hydrotreatment techniques [5-15]. With that, three main methods, such as hydrogenolysis, catalytic cracking and thermal cracking were deeply investigated. Hydrogenolysis produces long straight-chain hydrocarbon with a high cetane index, while cracking produces straight-chain hydrocarbon with by-products of lighter hydrocarbons and aromatics which were in the range of gasoline and fuel gas [16].

During triglycerides hydrogenolysis, catalytic hydrodeoxygenation (HDO) produce n-octadecane (C_{18}) in organic liquid products (OLP). Also, decarboxylation (DCO) (by-product as CO_2) and decarbonylation (DCA) (by-product as CO) are the side reactions, which produce n-heptadecane (C_{17}) [3-11, 15-18]. This study have been collectively involved in HDO, DCA and DCO of triglyceride in the presence of H_2 and named as hydroprocessing of vegetable oil [3-11]. At the hydroprocessing condition, (i.e.) between operating temperature of 300 to 400ºC and pressure of 1.0 to 10.0 MPa, solid catalyst on HDO was extensively studied in the literature [15-18]. Here, OLP may also contain traces of saturated and unsaturated hydrocarbons of acid, ester, alcohol, aldehyde, ketone in aromatic and aliphatic structure.

Recently, number of studies in the literature have investigated with catalytic effect over sulfide or non-sulfide form of mono- or bi-metals over the metal oxides like Al_2O_3, SiO_2, activated carbon, alumino-silicates and zeolite [14-24]. In few studies, activated carbon has been investigated over methyl or ethyl esters, which produced low pour-point property of diesel-like fuel, but had higher reaction rate on DCA than HDO [15-17].

High catalytic activity, high turnover frequency of active sites, chemical stability and a known quantity of catalysts requirement are mainly successful with the use of sulfiding transition metals. Here, substituting sulphur in feed for co-processing diesel and fatty acids makes additional operating cost [22, 23]. However, sulphur on mono- or bi-metallic transition metals on the support metal-phosphide and metal-carbide were extensively investigated in hydroprocessing conditions [21, 25].

**email: shapal.chem@kongu.edu*

If sulphur substituent concentration in the feed increases, the sulphur bounded bi-metallic transition metals (M-S) showed stable and high activity. In the case of absence of sulphur in the feed, active metal sites can be deactivated at a faster rate because of feed leaches M–S on active site by water formation. Sulfide catalyst has higher activity on metal-phosphide and metal-carbides support, but it was expensive due to the preparation and transformation of active catalyst [19, 28]. Similarly, Langmuir IV-isotherm adsorption type Ni-PTA/Al_2O_3 had given better yield and selectivity [24]. The presence of selective alumina as support had higher product selectivity and less cracking as compared to SiO_2 [23-26]. So, economically viable catalyst without sulphur-bound are extensively searched recent years.

In the search of sulphur-free catalyst, there were possibilities to use alumino-silicates or zeolites, such as Zeolite Socony Mobil (ZSM), mesoporous zeolite (SBA), Hydrogen-Beta (H-β), Y-type (H-Y), Silicoaluminophosphate (SAPO) and Mobil Composition Materials (MCM) in catalytic hydrotreatment of vegetal oil [18]. These materials with significant metal loads, are mainly involved in HDO and branching of hydrocarbon chains (they reduce cold flow plugging point) [25]. The recent study shows that substituting transition metals in lattice structures has increased the reactivity of catalyst, with slow deactivation at mild and moderate temperatures [24, 28]. In estimating the selectivity of HDO in compared to DCO and DCA products, the metals like Ni, Pd and Pt are more suitable [26, 29-31]. Like γ-Al_2O_3, the study mainly reveals that the zeolite-type metal oxides could be thermally stable, enhancing branching in hydrocarbon and increasing HDO yield. In this context, zeolite-type catalyst might be suitable for catalytic hydrotreatment of raw vegetal oil. The utilization of excess H_2 enables the slow deactivation and coking, where continuous H_2O production, as a by-product in HDO, reduces the leach over the active metals on catalyst surface and make way for C-O bond breaking in triglycerides [30, 31]. And also, absences of H_2 in thermal cracking of vegetable oil had produced esters, which reduce the reaction rate and yield [26].

Excluding mono-metallic catalyst, the recent study conducted with bi-metallic catalyst involved shorter reaction time and better selectivity [26, 29]. In this series, selecting two transition metals (bi-metals) with positive reduction potential on catalyst surface can effectively increase the HDO selectivity and activity. Sulphur-free metal catalysts with the reduced state can avoid sulphur contamination in the hydroprocessing product, but enhances DCA and DCO mechanism. Though less consumption of H_2 in DCO and DCA were theoretically economically compared to HDO, sulphur-free catalyst can adapt and does not contaminate the product by sulphur leaching [26]. Pt can emphasis the reduction of hydrocarbon and Pd can increase the capability of H-proton donor potential due to the strong interaction of Pd atom with the zeolite atoms. Both Pt and Pd are recommended to be used as a sulphur-free catalyst for investigating hydrotreatment of vegetal oil [26].

This work investigates the performance of sulphur-free bi-metallic catalysts, such as Pt and Pd on alumina zeolite (Pt-Pd/γ-Al_2O_3-H-β) NiMo/γ-Al_2O_3 and Pd/C, at 320°C and 2.0 MPa, in a semi-batch process. The study focus on HDO and DCA mechanism in OLP and the composition of fuel gas in the gas outlet.

2. Materials and methods

2.1. Materials

The pure triglyceride as refined from sunflower oil (SVO), purchased in a retail shop, contains no free fatty acids. The methyl oleate (98% from Sigma Aldrich) as model FAME compounds, n-dodecane (99% from Sigma-Aldrich) as solvent and n-tetradecane (99% from Sigma-Aldrich) as an internal standard of the sample were used. The catalyst used for the investigation was NiMo/Al_2O_3 (Criterion catalysts), its commercial name being Trilobe HDN-60, 5 wt% Pd on activated Carbon (lot number: 205680 from Sigma-Aldrich) as named Pd/C, and Beta zeolite in H-form, named as H-β (Product no: CP811C-300 from I*nternational zeolite corp. USA*) with SiO_2/Al_2O_3 mole ratio of 300 and 0.05 wt% of Na_2O. High purity of Boehmite Alumina Hydrates (as trade name disperal) was purchased from Sasol, Germany and $Pt(NH_3)_4Cl_2$ solution was purchased from Sigma-Aldrich. Boehmite Alumina Hydrates is used for the extrusion and $Pt(NH_3)_4Cl_2$ solution was used as Pt load on the zeolite.

2.2. Catalyst activation

The $NiMo/Al_2O_3$ contains 2-3 % Ni, 12-14 % Mo and 83-86% γ-Al_2O_3 support, extrudes at the sieve range of 10-30 DIN (aperture ~ 0.2-0.6 mm), for investigation of both sulphide and sulphide-free form of hydroprocessing catalyst. With reference to the previous studies, the sulphide form of $NiMo/\gamma$-Al_2O_3 (NiMo-S), calcined at 400°C, and *in-situ* sulphidation was carried out with 10% by volume of S in H_2S at 200 mL/min, for 3 h, in the trickle-bed reactor [6, 11] and a sulphide-free form of $NiMo/\gamma$-Al_2O_3 (NiMo) carried *in-situ* activated in H_2, at 400°C. Similarly, the Pd/C was activated with H_2 after drying in an oven at 110°C for 4 h. The catalysts were kept under an N_2 atmosphere to prevent from oxidation.

H-β and disperal (boehmite) were blended in a ratio of 40:60 wt%, and the hydrated blend was extruded in 1/32" and dried at 110°C, for 5 h. After calcination at 300°C for 4 h, 0.5 wt% of Pd and 0.5 wt% of Pt with respect to weight of support material (dry basis) are loaded on the extruder by wet impregnation method using $Pt(NO_3)_2.2H_2O$ and $Pd(NO_3)_2$ solution. Finally, the zeolite loaded with Pd and Pt (Pt-Pd/ γ-Al_2O_3-H-β) was calcined at 400°C for 6 h. The Pt-Pd/ γ- Al_2O_3-H-β was crushed and sieved in 10-30 DIN, and H_2 *in-situ* activation performed as like Pd/C and NiMo catalysts.

2.3. Reactor

The semi-batch reactor consists of a stainless steel vessel of 300 mL capacity. The reactor was connected with both inlet and outlet gas line. It consists of an eight-microprocessor based process controller with an integrated part to the thermocouple, heating mantle and magnetic stirrer [6]. After the catalyst activation, 1 g of catalyst taken in the vessel with a 150 mL solution containing 20 wt% of SVO in n-dodecane and 3 g of n-tetradecane as an internal standard [6]. The experiments were carried out from 320 and 340°C at 2 MPa, with the same stirring speed. Sampling point was connected at a gas outlet connection and an average of 1 mL of liquid sample (OLP) was extracted and stored in the 6°C cooler for analysis.

2.4. Physico-chemical characterization

The specific area and pore volume of the samples were analysed using Tristar 3000 automated Gas Adsorption Analyzer, measured by N_2 physisorption isotherms at -195°C. Before the analysis, 1 g sample of catalyst was thermally dried in a vacuum chamber, at 90°C for 4 h, in N_2 gas flow and used for specific surface area and pore-volume measurements.

The spent catalyst was refined for 22 h to extract the solvent, using m-xylene in the Soxhlet apparatus. The refined spent catalyst was dried in a vacuum dryer at 125°C under N_2, followed by the analysis of coke deposition by BELAB AB, Sweden, using an ASTM D5291 standard test method (*Leco CHN-600* instrument).

Simple distillation of 500 mL of OLP sample distilled under N_2 atmosphere (100 mL/min), at two desirable cut-off temperatures, i.e. 100 °C to remove water molecules in distillate and 200°C to remove n-dodecane and lighter hydrocarbons in distillate and rest as residue. This distillation was performed to identify the water molecules formation and elemental analysis of OLP residues.

The Spectrum One from Perkin–Elmer Fourier Transform Infrared Spectroscopy (FTIR) was used to analyses OLP samples at room temperature. OLP sample is placed between two high purity NaCl salt plates (pair of demountable cell in 4 mm thickness) with care for ensuring that no air bubbles appeared and the reading noted for mid-infrared ranges from 4000 cm^{-1} to 400 cm^{-1}[7].

Based on simulated distillation methods of ASTM D2887 standard, OLP samples (5 μL) has injected in Varian 3400 Gas chromatography (GC), equipped with a packed column (10% silicon OV-101, 80–100 mesh, 1 m ×1/8"× 2.00 mm) and a Flame Ionization Detector (FID) and Varian 4279 integrator are used for data computing [7]. With the injector and detector temperature of 300°C, the column oven temperature raised from 40 to 325°C, at a heating ramp of 18°C/min and the final temperature has been maintained for 10 min.

The outlet gas from the reactor was analysed using the Clarus 500 GC online, connected with 600 link switch controllers, with the signal integrated to receive data. Gas analyser consists of inlet and outlet sampling valves, actuated by N_2 gas on 0.4 MPa, which analyses CO, CO_2, CH_4 and H_2 at Thermal Conductivity Detector (TCD) and hydrocarbons in FID[6, 7, 11]. Elemental analyses in OLP such as C, H and O under ASTM D5291 standard test method are performed at Karlshamn Kraft AB, Sweden. The traces of S, metals and salts are exempted in the analytical test [7].

Bruker 600 NMR spectrometer, containing a 5 mm diffusion probe, was used to analyse under 300 MHz for ^1H. Pretreatment of SVO carried in vortex mix of 0.2 g in 400 microliter of deuterated chloroform, and the sample has placed in a 5-mm diameter ultra-precision.

3. Results and discussions

The experimental investigation has been performed for Pd/C, bi-metallic catalysts like NiMo on alumina and PtPd on the alumina-zeolite.

Table 1. Characterization of zeolite molecular size and extruded catalyst, determined by N_2 sorption, using the BET method

Material	Surface area (m^2/g)	Pore volume (cm^3/g)	Average pore width (Å)	Adsorption average pore diameter[a] (Å)	Desorption average pore diameter[b] (Å)	Coke db[c] (ASTM D5373)
Pd/C	935.7	0.22	31.8	51.0	48.4	**
NiMo/Al_2O_3	157.6	0.34	87.0	75.6	64.2	0.09
H-β	383.1	0.32	33.6	53.4	49.3	**
Extruded H- β	236.0	0.24	40.8	54.2	48.7	0.1
Spent-NiMo-S	54.5	0.12	89.5	69.6	51.1	2.1
Spent-Pt-Pd/γ-Al_2O_3-H-β	140.8	0.14	38.5	44.3	40.2	2.0

[a] Estimated from the adsorption branch of the isothermal N_2 sorption, using the BJH method.
[b] Estimated from the desorption branch of the isothermal N_2 sorption, using the BJH method.
[c] Analyzed by BELAB AB, Sweden, ASTM D 5291 standard test method. db=dry basis.

The pore size of the investigated catalysts, as shown in Figure 1 and Table 1, appears at the range between 50 Å and 80 Å. Mainly, NiMo has an average adsorption pore diameter of 75.65 Å and Pt-Pd/ γ- Al_2O_3-H-β had 54.24 Å. Pd/C had an average adsorption pore diameter of 51.03 Å. However, Pd/C in HDO might have a DCA/DCO mechanism with intermediates of oleate or stearaldehyde, and HDO can be enhanced with active sites using a fresh H_2 supply. But, coke deposition over active sites can harm the activity and performance of catalyst life-span. On this NiMo regeneration ability, coke deposition over catalyst can deteriorate pore mouth shrinking and decreases the surface area. The spent NiMo-S average adsorption pore diameter was 64.2 Å, and the surface area was 54.5 m^2/g, whereas fresh NiMo-S had 157.6 m^2/g. The trend of N_2 absorption and desorption appeared as Langmuir type IV isotherms for both fresh (Figure 1) and spent catalyst, but the quantity of adsorption diminished with the coke deposition. The total pore volume for adsorption of fresh and spent catalyst reduced from 0.34 cm^3/g to 0.12 cm^3/g. Hence, the coke deposits might be involved in the rupture of S-metal and further formation of hydrogen sulphide had been reduced to a fresh supply of sulphur and hydrogen for the active sites. From the literature, it is evident that the moderate pore size of NiMo-S, NiMo and Pt-Pd/ γ-Al_2O_3-H-β catalysts can control the secondary cracking [29]. Langmuir adsorption isotherms is used to investigate different materials are indicated in Figure 1, in which the hydroprocessing study of Pt-Pd/ γ-Al_2O_3-H-β reduces the pore diameter of 69.6 Å to 44.3 Å. The result of lower coke deposition in Pt-Pd/ γ- Al_2O_3-H-β was an indication of a lower rate of deactivation and also, the selectivey and yield indicator of the HDO can be used as the study for the catalyst performance.

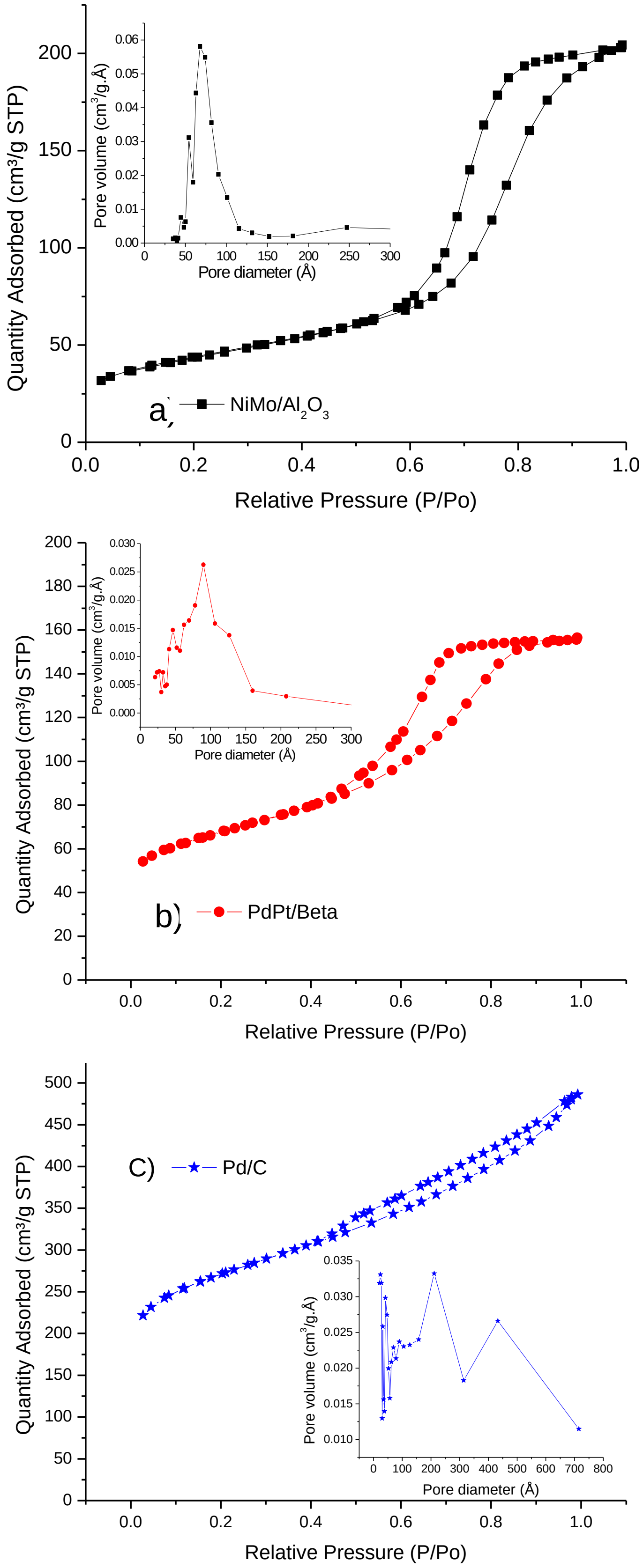

Figure 1. Surface area and pore volume characterization of the fresh catalysts
a) NiMo-S/Al_2O_3, b) Pt-Pd/ γ- Al_2O_3-H-β and c)Pd/C (Note: NiMo/Al_2O_3 and
b) PdPt/Beta are denoted for NiMo-S/Al_2O_3 and Pt-Pd/ γ- Al_2O_3-H-β in graphical representation)

3.1. Oxygenated products

The study examined over triglycerides hydrogenation and HDO using NiMo, NiMo-S, Pd/C and Pt-Pd/γ- Al_2O_3-H-β, which are carried out at 320°C and 2.0 MPa, either in the absence or presence of H_2. As there are different materials with different shapes and structures in these catalyst studies, it is required to identify the minimum mass transfer resistance [32]. So, the effect of mass transfer resistance on the external catalyst surface can be determined by performing different temperatures and sterrier speeds. The conversion rate for 3 h run in batch reactor, for 20 wt% vegetal oil (20-SVO) in n-dodecane solvent of 320°C and 2.0 MPa shows identical product formation at 650 rpm to 1000 rpm. The sterrier speed of 700 rpm is used for all the test-run with understanding of negligeble external diffusion, which has not influence the rate-controlling step. Also, under similar condition, hydrogenolysis of SVO is investigated. In this examining, for 10°C raise in operating temperature (between 300 and 35°C), it tends to double the HDO conversion rate. This indicates the negeligible pore diffusing effect over the catalyst surface [31,32].

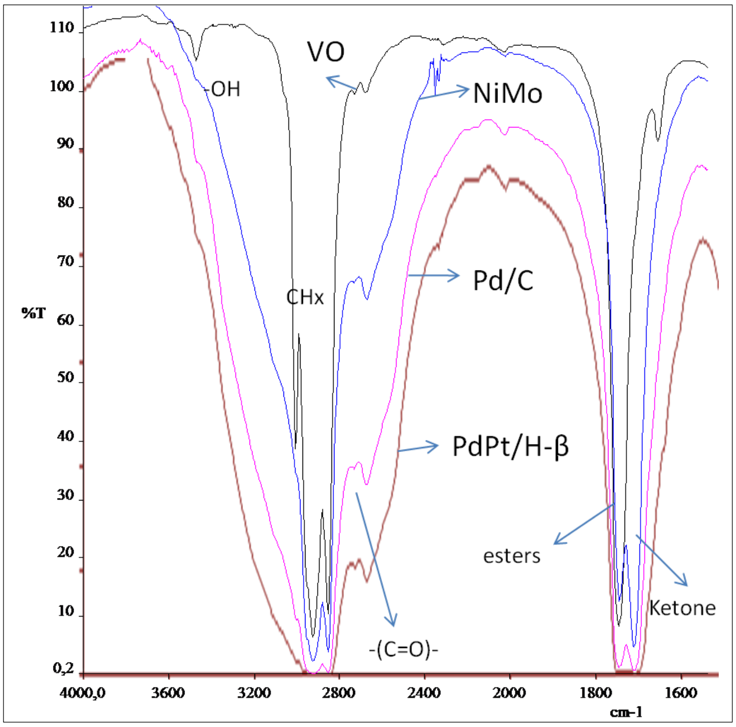

Figure 2. FTIR analysis of hydroprocessing pure sunflower oil samples with (NiMo)NiMo-S/Al_2O_3, Pd/C and Pt-Pd/ γ- Al_2O_3-H-β at T= 320 °C and 2.0 MPa (residence time 60 min)

The formation of oxygenated compounds, such as esters, carboxylic acids, aldehydes or ketones in OLP, appeared by the dissociation of –C–O– in glycerides and –C–O–(CO)– into free fatty acid/aldehydes and glycerol [15-20]. Figure 2 and 3 at FTIR transmission mode indicate the functional group appeared in the OLP.

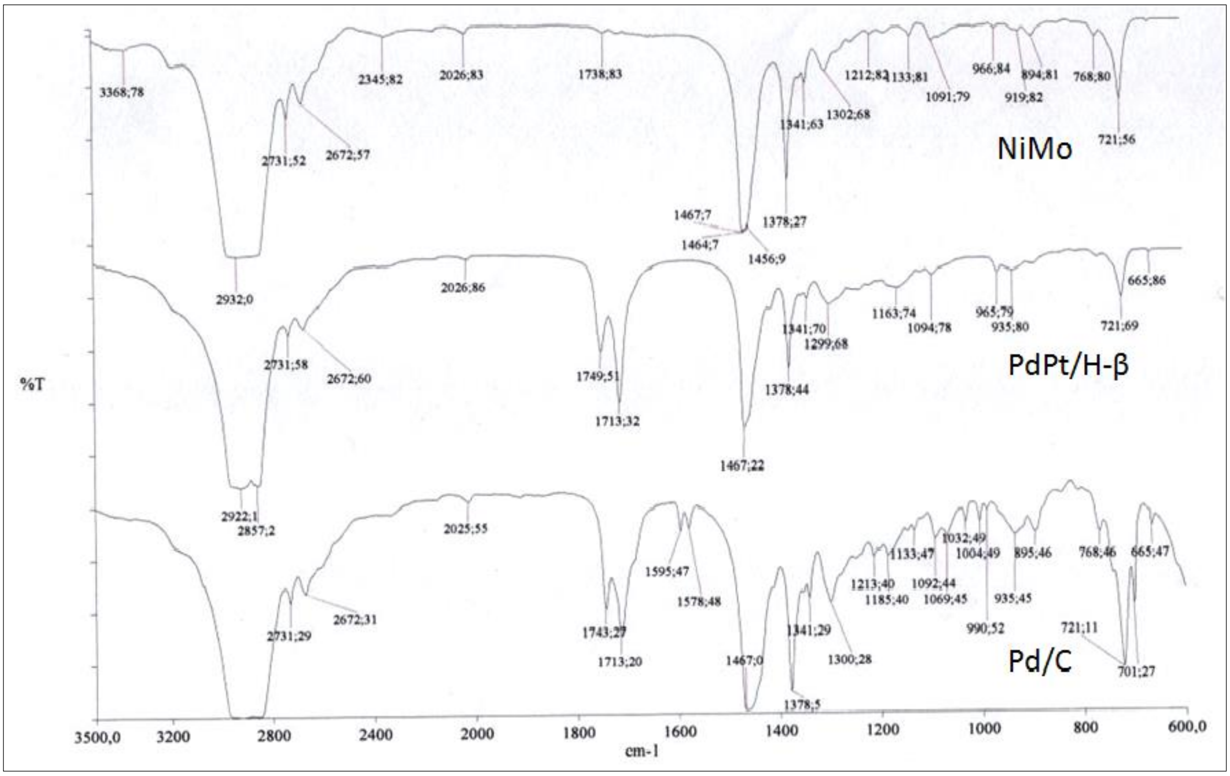

Figure 3. FTIR analysis of hydroprocessed 20-SVO after distilled (at operating condition: T=320 °C, P=2.0 MPa and 100% conversion of triglycerides) samples taken on residence time in semi-batch reactor: NiMo= 150 min, Pt-Pd/ γ- Al_2O_3-H-β=120 min and Pd/C=150 min

The FTIR result (Figures 2 and 3) observes that the aldehydes and alcohol formation shows an increase in concentration, at a wavelength between 2800 cm^{-1} and 3100 cm^{-1}, which mainly shows the CH_X level of the fatty ester group by HDO. A wavelength of about 3200 cm^{-1} - 3400 cm^{-1} shows the presence of carboxyl acids (-(C=O)-OH) or alcohol (O-H) or water molecules. The wavelength around 2731 cm^{-1} shows the formation of aldehyde or ketone group and a peak at 1713 cm^{-1} - 1715 cm^{-1} wavelength shows the presence of carboxyl acids or carbonyl compounds, represented in C=O stretching. The wavelength peak at 1748 cm^{-1} -1742 cm^{-1} in catalytic hydroprocessing indicates the formation of esters and a peak at 920 cm^{-1} indicated the appearance of the aromatic and dimer group. Here, the radicals of carboxylic esters could form dimer compounds and it can be confirmed at the wavelength of 1280 cm^{-1} and an increase in C=C stretch at 1650 cm^{-1}, as observed in Figure 3. The dimers from the polymerisation of the carboxyl group show high concentration intensity for Pd/C, but other catalysts show only traceable amount. The band identified functional groups are listed in Table 2 based on using studies carried by Tegou et al [33].

Table 2. Characterization of notable band assignment in OLP from catalytic treatment with thermal decomposition as the wavelength collected from Figures 3 & 4 and its band identification.

Wave length (cm^{-1})				Band assignment
NiMo-S	Pd/C	Pt-Pd/γ-Al_2O_3-H-β	Thermal cracking	
2932, 2731, 1467	2922, 2731, 1467	2922, 2731, 1467	2730	Symmetric and asymmetric stretching vibration of the aliphatic CH_2 group, alkenes
2672	2672	2672	2800	aldehyde C-H, acids O-H (very broad)
1738	1749	1743	-	C=O, aliphatic esters, ester carbonyl group
1341	1713, 1341	1713, 1341	1710	C=O stretching, -COOH, Free fatty acids
-	1595, 1578	-	1595, 1578	C=C (in ring) (2 or 3 bands), arenes

1378	1378	1378	-	Bending vibrations of CH_2 groups
1302	1299	1300	-	C-O (alcohol)
1091	1092, 1069	1163, 1094	-	C–O stretching (α-hydroxyl), stretching vibration of the C-O ester groups
-	1032	-	-	C–O stretching (β-hydroxyl)
966	-	965	966	*trans*-R-CH=CH-R’
919, 721	939, 721	939, 721	-	CH_2 rocking
-	701	-	-	Arenes
-	665	665	-	*cis*-R-CH=CH-R’

To understand thermal cracking in the catalytic hydrotreating technology, a non-catalytic thermal treatment needs to be carried out. Thermal cracking of 20-SVO triglycerides at 320 ºC and 2.0 MPa in N_2 atmosphere is investigated and table 2 represents the identified major spectroscopy peak. The wavelength of 1710 cm^{-1} indicates the carbonyl structure, either –(CO)H or –(CO)–. Also, the wavelength of 2730 cm^{-1} implies the aldehydes or ketones, which show a broader spectrum indication. These broadband wavelengths of 2730 cm^{-1} and 1710 cm^{-1} show the formation of carboxyl acids that was due to the α-carbon bond dissociation from the propane group. The FTIR result shows that wavelength from 3010 cm^{-1} to 2800 cm^{-1} has a broad intensity as noticed in Figure 3. This more widespread intensity denotes the presence of a high concentration of glycerol or hydroxyl group, because of CH_x scission between α- and β-carbon in glyceride ester. The C-O bond of glyceride breaks at low enthalpy by leaving aldehyde or acid, or by leaving the both. In the Pd/C hydrotreatment, the intensity in the OLP sample at 1595 cm^{-1} and 1578 cm^{-1} indicates aromatic/cyclic compounds. These arene compounds formation from the coupling of α-carbon radical and carbonyl group are either formed from ester or propane dissociation in glycerides. The aromatic/cyclic compounds, as indicated by the wavelength of 1032 cm^{-1} and 701 cm^{-1}, confirmed the presence of β-hydroxyl carbonyl compounds. Table 2 reports the band assignment in OLP and the carboxylic and carbonyl compounds for all the tested catalysts that had resembled in HDO product formation and also its reaction route. Table 2 and Figure 3 show the presence of *trans*- and *cis*- hydrocarbon chain. PdPt//γ-Al_2O_3-H-β has the strong and moderate intensity of *trans*- and *cis*- hydrocarbon, NiMo-S has only strong intensity at 966 cm^{-1} indicating *trans*-alkenes and Pd/C has strong intensity at 665 cm^{-1} reporting *cis*-alkenes, whereas thermal cracking of *trans*-alkenes are observed on strong intensity at 966 cm^{-1}, however, in the presence of H_2 at thermal cracking induces in *cis*-alkenes formation.

It is found that the products from thermal treatment initiate bond breaking on esters. The breakage of the –C–O– bond, either on the glycerol or ester chain can be expected. Primarily, the thermal vibration over the C-C bonding initiates the decomposition of the saturated structure rather the unsaturated group. So, C=O and C=C has the stability on high bond energy [34] and inhibits secondary cracking on the saturated group; this implies that the catalytic activity can induce the carbonyl or pi-bonding at the active sites. The α-carbon had weak stability and had low bonding energy, when compared to the β-carbon with its adjacent, so β-carbon can withstand the bond breaking to its adjacent of α-carbon and γ-carbon compounds, as also mentioned in [35]. Thus, the expected bond break in α-carbon can produce radicals which can saturate its valence using abstraction of –H atom from near-by carbon or in the hydrocarbon chain. This abstraction induces the unsaturation in the hydrocarbon between C_3 and C_{15} carbon chains, and this can also initiate aromatic or cyclic compound formation.

3.2 Hydrogenation and Hydrogenolysis

In H_2 atmosphere, pure SVO and 20-SVO in a semi-batch reactor are tested at 320ºC and 2.0 MPa by NiMo-S, Pd/C and PdPt//γ-Al_2O_3-H-β catalysts. Here, the sampling of SVO hydroprocessed has tested with ^{1}H-NMR, which indicated the formation of hydrocarbons of C_{17} and C_{18} in hydroprocessing. This can be noticed in Figure 4. The peak identified ^{1}H-NMR at 2.5-3 f1(ppm) for glycerides are disappeared in the OLP. It is revealed that the hydrogenation of the triglycerides formed, initially. Dissociation of carboxyl compounds initiates, and further the formation of saturated C_{17} and C_{18} hydrocarbons can be proved as the desired products of glycerides hydrogenolysis.

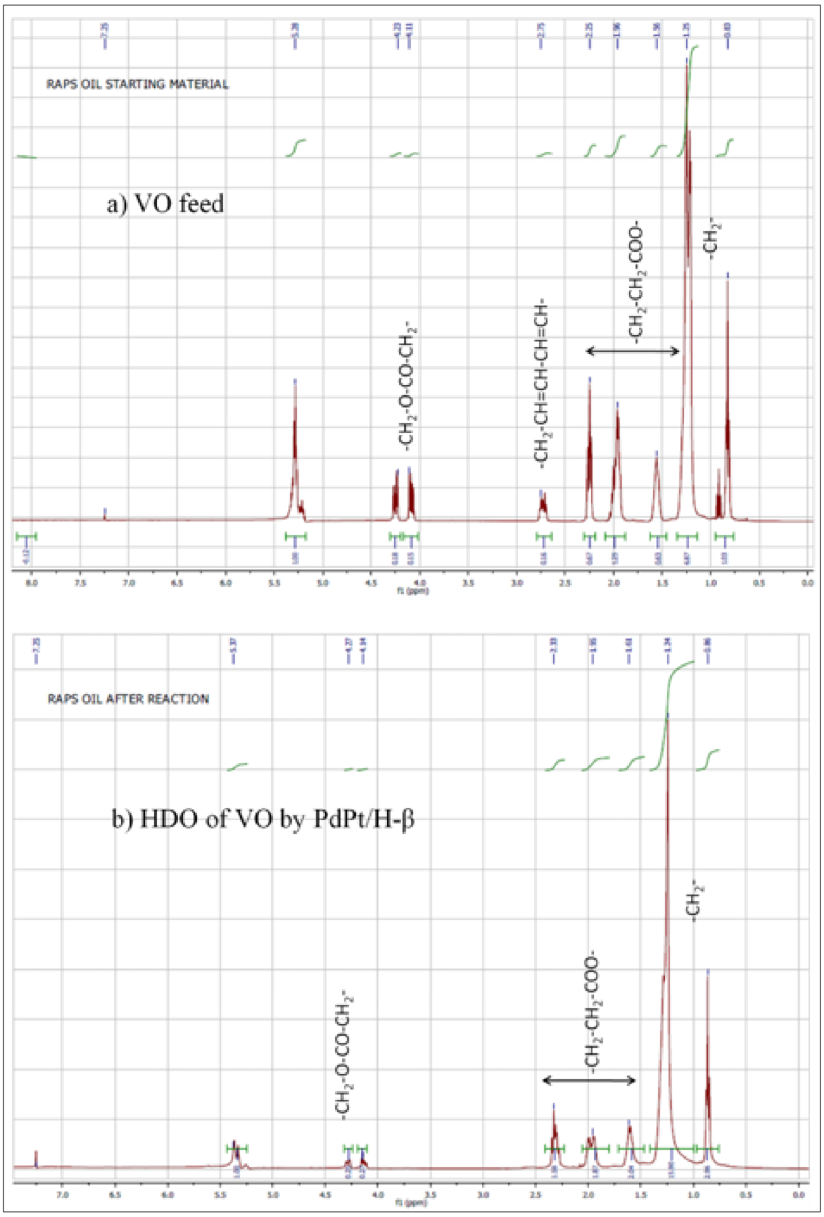

Figure 4. 1H-NMR spectra (300 MHz for 1H) of a) feed SVO and b)SVO hydroprocessed using Pt-Pd/ γ- Al_2O_3-H-β at T= 320 °C and 2.0 MPa for 120 min

The composition of carboxylic compounds in the intermediates using Pd/C and Pt-Pd/γ-Al_2O_3-H-β catalytic process shows a side reaction in the formation of esters, carbonyl, carboxylic and lighter hydrocarbons (less than C_8) in the OLP, as shown in the Figure 5 and 6. But, SVO HDO by NiMo-S shows the highest yield in obtaining C_{17} and C_{18} hydrocarbons with minor quantity of carbonyl compounds. Product selectivity is reduced due to a low partial pressure of H_2 in the involvement of –H protonation in the deoxygenation mechanism. Metal loaded on the catalyst was mainly beneficial for proton donor of DCA/DCO. While substituting of –H donor on HDO for carbonyl compounds results in the formation of water molecules and hydrogenolysis compounds such as (both saturated and unsaturated) C_{18}. The abstraction of –H from hydrocarbon gives additional protonation on metal sites [7, 11]. But, lower electrophilicity on Ni metal over Mo, results in favour of HDO rather than direct scission of (C=O)–O and C=O bonds. Further sulphides improved the deoxygenation by metal effects, like Ni dispersion, and they gains direct deoxygenation with high selective compounds in hydroprocessing.

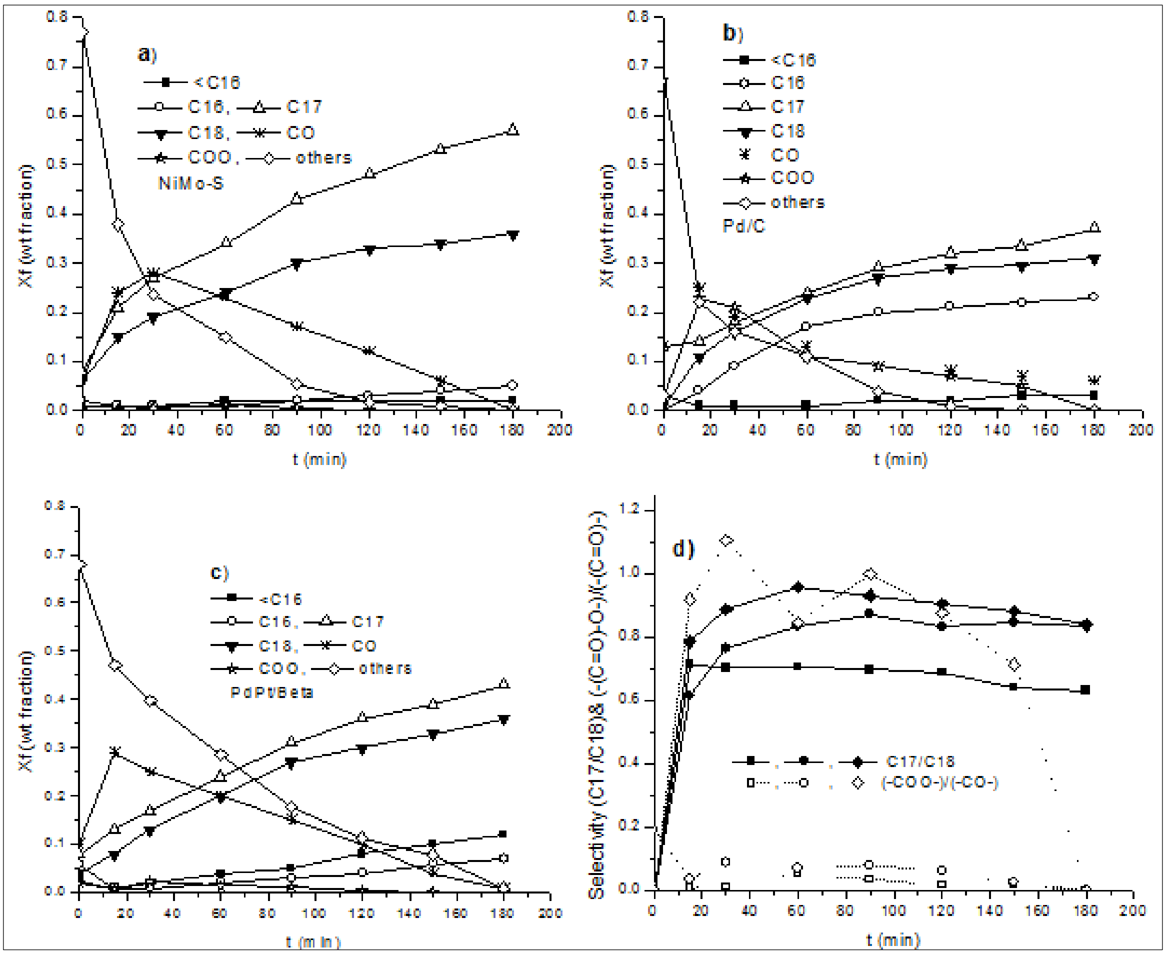

Figure 5. Concentration profile of OLP from hydroprocessing sunflower oil at 320 ^{o}C, 2.0 MPa with a) NiMo-S, b) Pd/C, c) Pt-Pd/γ-Al_2O_3-H-β catalyst and d) Selectivity of C_{17}/C_{18} and carboxylic acid (-COOH-)/carbonyl aldehyde (-CO-) represented as □ & ■-NiMo-S, ○&●- Pd/C and ♦ &◊- Pt-Pd/γ- Al_2O_3-H-β. (Note: PdPt/Beta denoted as Pt-Pd/γ-Al_2O_3-H-β).
(lines are drawn to guide eye)

In using PtPd/H-β, the formation of both straight- chain and branched C_{17} and C_{18} from hydrogenating carbonyl compounds are noticed. The deoxygenation associated with branching of hydrocarbon can be expected for hydroprocessing with the support of zeolite. Similarly, this branching can confirm with the higher unsaturated gases hydrocarbon such as ΣC_3, ΣC_4 and ΣC_5 mentioned in the Figure 6. However sulfur-free catalyst of Pt-Pd/γ-Al_2O_3-H-β has weak acidity to undergo for deoxygenation with proton donor of –H atoms and the role on surface area and specific hydrogenation metals induces hydrogenolysis. This hydrogenation and hydrogenolysis are the primary reaction mechanism involved in hydrotreating and, collectively, this catalytic and thermal hydrotreating undergones hydroprocessing in the production of renewable diesel.

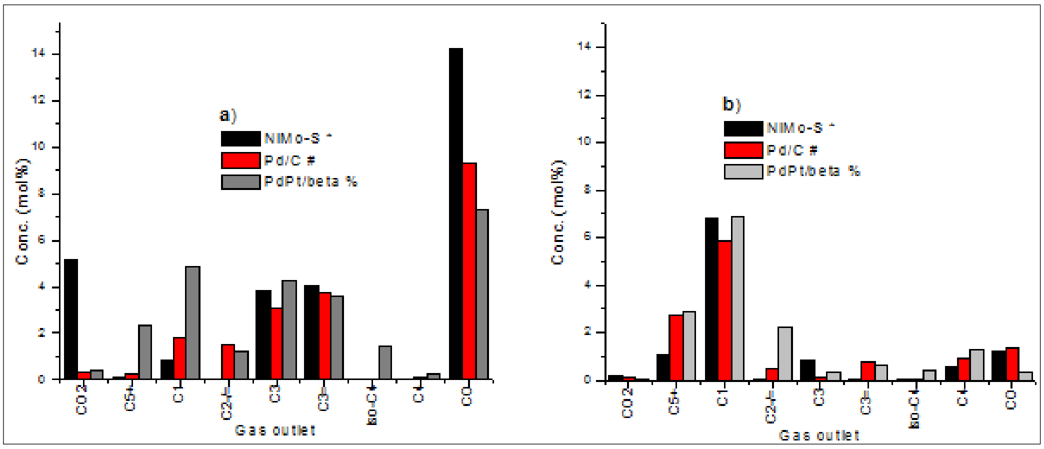

Figure 6. Concentration profile of gas outlet at T= 320°C, 2.0 MPa, with (*)NiMo-S, (#)Pd/C and (%) Pt-Pd/γ-Al_2O_3-H-β catalyst for hydroprocessing a) sunflower oil and b) methyl oleate (Note: PdPt/Beta denoted as Pt-Pd/γ-Al_2O_3-H-β)

3.3 Catalytic hydroprocessing of triglycerides

The hydroprocessing of the triglycerides with saturated and unsaturated C_{18} compounds examined at temperature 320°C and 2.0 MPa represented in Figure 5. The notable results in Figure 5 shows that the formation of intermediate such as carboxylic acid (C_{17}-COOH), ketones and aldehydes (C_{17}-CO-). So, this intermediate produces C_{17} and C_{18} saturated hydrocarbons. Figure 5b indicates the actual product distribution in OLP for Pd/C hydroprocessing. The decomposition of C_{17}-COOH or C_{17}-CHO formed C_{16} and C_{17} in the OLP with partial hydrogenation and, this by-product can produce CO, CO_2, methane (C_1) and ethane/ene in the gas outlet. The total concentration of CO, CO_2, C_1 and ethane/ene have produced 20, 13.5 and 14 mol% at gas outlet through decomposition mechanism in NiMo-S, Pd/C and Pt-Pd/γ-Al_2O_3-H-β, has been observed in Figure 6a. Also, the same condition at MO has produced total concentration of CO, CO_2 and ethane/ene are 2.44 mol%, 2.26 mol% and 2.27 mol%, has been observed in Figure 6b. These results confirm the C-C cracking of α- and β-carbon at fatty acids. The CO and CO_2 in DCO and DCA mechanism evolved from hydrotreating of glycerides and it can also reduce the cetane value of diesel [36].

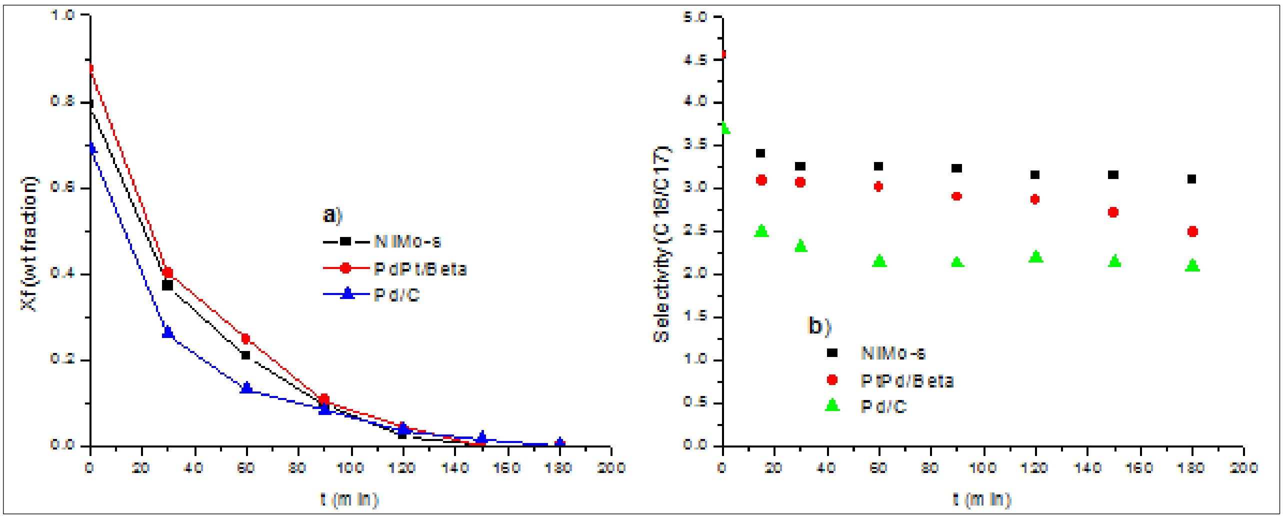

Figure 7. Product from HDO of MO in OLP sample at T= 320 °C and 2.0 MPa for Catalytic hydroprocessing: a) disappearance of MO and b) selectivity of C_{18}/C_{17}. Note: PdPt/Beta denoted as Pt-Pd/ γ-Al_2O_3-H-β. (lines are drawn to guide the eye)

The HDO of NiMo-S, Pd/C and Pt-Pd/γ-Al_2O_3-H-β have produced propane/ene from SVO, as the compositions of gases 8.2, 7.1 mol% and 8.1 mol%, while methane from MO gives the compositions of 7.0, 6.2 mol% and 7.1 mol%. The hydrogenation of CO and CO_2 into C_1 might happen in fuel gas of hydrotreatment. Using Pt-Pd/γ-Al_2O_3-H-β, the hydrogenation of CO and CO_2 to C_1 can attain hydrogenation at a low temperature over lower thermodynamically equilibrium condition. This driving mechanism might also enable the hydrogenation of CH_3-COOH and CH_3-CHO into ethane/ene. However, the selectivity of C_{17}/C_{18} mole ratio from triglycerides through both NiMo-S and Pd/C relatively appears between 0.7 and 0.85; Pt-Pd/γ-Al_2O_3-H-β can produce 0.95 as indicated in the Figure 5d. Similar comparison of results on the mol ratio selectivity of carboxylic to carbonyl hydrocarbon indicates the NiMo-S and Pd/C below 0.2, but Pt-Pd/γ-Al_2O_3-H-β shows nearly 1.1. The DCO and DCA mechanism in hydroprocessing produces C_{17}, whereas the rate of this mechanism on NiMo-S [7, 11] and Pt-Pd/γ-Al_2O_3-H-β may reduce the moderate temperature. This result confirms the formation of free fatty acids as intermediate and has a higher rate of C_{18} formed over sulphur-free zeolite. In the case of carbonyl group from glycerides, it induces higher decomposition to form C_{17}, CO and CO_2, thus the selectivity of C_{17}/C_{18} had lower value for NiMo-S and Pd/C. Especially, Pd/C has a higher rate of DCA and DCO reaction, which form low C_{18} hydrocarbons. With a lower selectivity ratio of C_{17} and C_{18}, the cetane value can be enhanced in renewable diesel. Figure 7a points out that the rate of disappearing of triglycerides was higher for Pd/C than other catalysts. But, its product selectivity is 20 to 30% lower than NiMo-S and Pt-Pd/γ-Al_2O_3-H-β, respectively, and this value can be observed in Figure 7b and Table 3. As compared to NiMo-S, Pt-Pd/γ-Al_2O_3-H-β has received 7% to 10% lower product selectivity in OLP, which indicates the branching of hydrocarbon tend to secondary cracking to form smaller fragment hydrocarbon. This hydrocarbon may not produce oligomeric products at the α-carbon of any hydrocarbon chain, for both OLP of 20-SVO and MO. Hence, in disproportion mechanism, product hydrocarbon contain branches have been suitable for diesel compounds if its carbon chain within in its composition and boiling point ranges has became an advantage. So, as indicate in Table 3, it indicates that the OLP have the formation of isomeric compounds using Pt-Pd/γ-Al_2O_3-H-β which is beneficial for fuel properties. Also, the low concentration of cyclic and aromatic compounds noted in zeolite HDO. But, the hydroprocessing of oxygenated hydrocarbon might need higher residence time for the complete hydration. So, it is necessary to have complete hydroprocessing with smaller flow velocity of direct SVO in continuous process.

Table 3. Hydroprocessing 20-SVO with different catalysts, at T= 340 °C and 40 bar. (Residence time in batch reactor for 120 min)

Products	**SVO (wt%)**				**MO (wt%)**			
	NiMo/ Al_2O_3	NiMoS/A l_2O_3	Pd/C	PtPd/γ-Al_2O_3-H-β	NiMo/ Al_2O_3	NiMoS /Al_2O_3	Pd/C	PtPd/γ-Al_2O_3-H-β
<ΣC_{16}	0.7	0	0.4	4.7	2.3	0.1	0	2.9
ΣC_{17}	1.6	10.8	9.3	5.1	3.1	8.2	8.9	5.3
ΣC_{18}	0.3	7.8	6.9	3.2	3.7	11.7	7.9	4.8
ΣC_{17}-CHO	3.5	1.4	2.7	4.4	4.3	0.1	3.1	6.4
ΣC_{17}-COOH	2.5	0.1	0.5	1.8	**	**	**	**
ΣC_{18}-OH	0	0	0.1	0	**	**	**	**
% Conv.	42.8	99.5	99.5	96.1	67.3	99.4	99.5	97.2

Initially, the hydroprocessing of SVO in the presence of H_2 has involved in the hydrogenation, rather than the effect of hydration, which happens if the saturation effectively consumes H_2. So, the rate of deoxygenation slows down due to weak –H proton density on the surface of active sites or inadequate H_2 supply through the gas film. However, the presence of –H proton on transition metals can suppress the dehydrogenation mechanism. So, suppressed dehydrogenation can critically affect the initiation of branching of the carbenium ions. But, in this study, the –H proton deficiency enhances the dehydrogenation and increases the carbenium formation. So, this mechanistic rate of hydrogenation and dehydrogenation can increase the carbocation and secondary cracking. In addition to partial hydrogenation, cracked hydrocarbon can consume H_2. In this case of reduced –H proton for longer residence time, the decrease in the slope of selectivity can be identified due to the catalyst proton deficiency, which is observed in Figure 7b. Hence, it increases the rate of dissociation, either the dehydrogenation from alcohol or DCO of carbonyl group into C_{17} and CO or CO_2.

4. Conclusions

This study reveals that C_{18} and C_{17} are the final products in hydroprocessing of all sulphide and non-sulphide catalysts, excluding high concentration of C_{16} formation in Pd/C. NiMo-S can achieve high catalytic activity and selectivity; instead, the use of NiMo can initiate DCA and DCO pathways only. The reduction of H_2 partial pressure involves in deactivation either by –S rupture on active sites or reduced dehydration with no proton supply in the HDO mechanism. So, H_2 consumption for hydrogenation of unsaturated glyceride ester group is notable for all tested catalysts. The unsaturated SVO contains mainly *cis*-group esters, which can be converted into trans-group esters. Multilayer adsorption over Pd/C catalyst involved in α- and β-carbon cracking as the intrinsic mass transfer control on the surface for desorption might break of the molecules into lighter hydrocarbon. Also, DCA and DCO can be extended to higher order in thermal dissociation due to smaller pore volume. Langmuir IV-type adsorption isotherm of catalysts such as NiMo-S and Pt-Pd/γ-Al_2O_3-H-β has enhanced HDO with higher pore volume, which can give better selectivity in C_{17} and C_{18} formation. However, Pt-Pd/γ-Al_2O_3-H-β resembles in the reaction rate with NiMo-S and forms relatively similar coke deposition and deactivation. Also, branching of carboxylic and carbonyl compounds in hydroprocessing through Pt-Pd/γ-Al_2O_3-H-β is beneficial, but higher temperature can induce the equilibrium and increases the decomposition at a disproportion route to make hydrocarbon branching such as isomerisation and oligomerisation.

Acknowledgments: We thank Dr. Borje S. Gevert for experimental support and special thanks to Preem AB, Sweden, for sample analysis.

References

1.DRAGOMIR, R.E., ROSCA, P. Biofuel from Hydroprocessing Fish Oil, *Rev. Chim.*, **71**(1), 2020, 176-185

2.JAMES, O.O., MAITY, S., MESUBI, M.A., USMAN, L.A., AJANAKU, K.O., SIYANBOLA, T.O., A review on conversion of triglycerides to on-specification diesel fuels without additional inputs, *International Journal of Energy Research*, 36(6), 2012, 691-702.

3.SANKARANARAYANAN, T.M., BERENGUER, A., OCHOA-HERNÁNDEZ, C., MORENO, I., JANA, P., CORONADO, J.M., Hydrodeoxygenation of anisole as bio-oil model compound over supported Ni and Co catalysts: Effect of metal and support properties, *Catalysis Today*, 243, 2015, 163-172.

4.PALANISAMY, S., GEVERT, B.S., SANKARAN, P., KANDASAMY, K., Produce low aromatic contents with enhanced cold properties of hydrotreated renewable diesel using Pt/alumina-beta-zeolite: Reaction path studied via mono-aromatic model compound, *Energies*, 12, 2019, 2853.

5.LIU, C., LIU, J., ZHOU, G., TIAN, W., RONG, L., A cleaner process for hydrocracking of jatropha oil into green diesel, *Journal of the Taiwan Institute of Chemical Engineers*, 44, 2013, 221–227.

6.PALANISAMY, S., GEVERT, B.S., Hydroprocessing of fatty acid methyl ester containing resin acids blended with gas oil, *Fuel Processing Technology*, 126, 2014, 435-440.

7.PALANISAMY, S., GEVERT, B.S., Study of non-catalytic thermal decomposition of triglyceride at hydroprocessing condition, *Applied Thermal Engineering*, 107, 2016, 301-310.

8.SHELDON, R.A., Green chemistry, catalysis and valorization of waste biomass, *Journal of Molecular Catalysis A: Chemical*, 422, 2016, 3-12.

9.TOBA, M., ABE, Y., KURAMOCHI, H., OSAKO, M., MOCHIZUKI, T., YOSHIMURA, Y., Hydrodeoxygenation of waste vegetable oil over sulfide catalysts, *Catalysis Today*, 164(1), 2011, 533-537.

10.ASIKIN-MIJAN, N., LEE, H.V., ABDULKAREEM-ALSULTAN, G., AFANDI, A., TAUFIQ-YAP, Y.H., Production of green diesel via cleaner catalytic deoxygenation of Jatropha curcas oil, *Journal of Cleaner Production*, 167, 2017, 1048-1059.

11.PALANISAMY, S., GEVERT, B.S., Hydrodeoxygenation of fatty acid methyl ester in gas oil blend–NiMoS/alumina catalyst, *Green Processing and Synthesis*, 7(3), 2018, 260-267.

12.FURIMSKY, E., Hydroprocessing challenges in biofuels production, *Catalysis Today*, 217, 2013, 13-56.

13.KORDULIS, C., BOURIKAS, K., GOUSI, M., KORDOULI, E., LYCOURGHIOTIS, A., Development of nickel based catalysts for the transformation of natural triglycerides and related compounds into green diesel: a critical review, *Applied Catalysis B: Environmental*, 181, 2016,156-196.

14.HANCSÓK, J., KRAR, M., MAGYAR, S.Z., BODA, L., HOLLÓ, A., KALLO, D., Investigation of the production of high quality biogasoil from pre-hydrogenated vegetable oils over Pt/SAPO-11/Al_2O_3, *Studies in Surface Science and Catalysis*, 170, 2007, 1605-1610.

15.ARORA, P., OJAGH, H., WOO, J., GRENNFELT, L.E., OLSSON, L., CREASER, D., Investigating the effect of Fe as a poison for catalytic HDO over sulfided NiMo alumina catalysts, *Applied Catalysis B: Environmental*, 227, 2018, 240-251.

16.SIMACEK, P., KUBICKA, D., SEBOR, G., POSPISIL, M., Hydroprocessed rapeseed oil as a source of hydrocarbon-based biodiesel, *Fuel*, 88(3), 2009, 456-460.

17.JENISTOVA, K., HACHEMI, I., MÄKI-ARVELA, P., KUMAR, N., PEURLA, M., CAPEK, L., Hydrodeoxygenation of stearic acid and tall oil fatty acids over Ni-alumina catalysts: Influence of reaction parameters and kinetic modelling, *Chemical Engineering Journal*, 316, 2017, 401-409.

18.BUZETZKI, E., SIDOROVA, K., CVENGROSOVA, Z., KASZONYI, A., CVENGROS, J., The influence of zeolite catalysts on the products of rapeseed oil cracking, *Fuel Processing Technology*, 92(8), 2011, 1623-1631.

19.WANG, H., YAN, S., SALLEY, S.O., NG, S.K.Y., Support effects on hydrotreating of soybean oil over NiMo carbide catalyst, *Fuel*, 111, 2013, 81-87.

20.KROBKRONG, N., ITTHIBENCHAPONG, V., KHONGPRACHA, P., FAUNGNAWAKIJ, K., Deoxygenation of oleic acid under an inert atmosphere using molybdenum oxide-based catalysts, *Energy Conversion and Management*, 167, 2018, 1-8.

21.ZHANG, W., YE, Z., ZHAO, L., WEI, W., Catalytic Activities of NiMo Carbide Supported on SiO_2 for the Hydrodeoxygenation of Ethyl Benzoate, Acetone, and Acetaldehyde, *Energy & Fuels*, 24(3), 2010, 2052-2059.

22.SINHA, A.K., SIBI, M.G., NAIDU, N., FAROOQUI, S.A., ANAND, M., KUMAR, R., Process Intensification for Hydroprocessing of Vegetable Oils: Experimental Study, *Industrial & Engineering Chemistry Research*, 53(49), 2014, 19062-19070.

23.ZHAO, Y., PRINS, R., Mechanisms of hydrodenitrogenation of alkylamines and hydro-desulfurization of alkanethiols on NiMo/ Al_2O_3, CoMo/ Al_2O_3, and Mo/ Al_2O_3, *Journal of Catalysis*, 229(1), 2005, 213-226.

24.LIU, J., LEI, J., HE, J., DENG, L., WANG, L., FAN, K., Hydroprocessing of Jatropha Oil for Production of Green Diesel over Non-sulfided Ni-PTA/ Al_2O_3 Catalyst, *Scientific Reports*, 5, 2015,11327.

25.WANG, F., JIANG, J., WANG, K., ZHAI, Q., SUN, H., LIU, P., Activated carbon supported molybdenum and tungsten carbides for hydrotreatment of fatty acids into green diesel, *Fuel*, 228, 2018,103-111.

26.WANG, C., LIU, Q., SONG, J., LI, W., LI, P., XU, R., High quality diesel-range alkanes production via a single-step hydrotreatment of vegetable oil over Ni/zeolite catalyst, *Catalysis Today*, 234, 2014, 153-160.
27.SRIFA, A., FAUNGNAWAKIJ, K., ITTHIBENCHAPONG, V., ASSABUMRUNGRAT, S., Roles of monometallic catalysts in hydrodeoxygenation of palm oil to green diesel, *Chemical Engineering Journal*, 278, 2015, 249-258.
28.SÁNCHEZ, M.J.F., BOLDRINI, D.E., TONETTO, G.M., DAMIANI, D.E., Palladium catalyst on anodized aluminum monoliths for the partial hydrogenation of vegetable oil, *Chemical Engineering Journal*, 167(1), 2011, 355-361.
29.LUP, K.A.N., ABNISA, F., WAN DAUD, W.M.A., AROUA, M.K., A review on reactivity and stability of heterogeneous metal catalysts for deoxygenation of bio-oil model compounds, *Journal of Industrial and Engineering Chemistry*, 56, 2017, 1-34.
30.SATYARTHI, J.K., CHIRANJEEVI, T., GOKAK, D.T., VISWANATHAN, P.S., An overview of catalytic conversion of vegetable oils/fats into middle distillates, *Catalysis Science & Technology*, 3(1), 2013, 70-80.
31.CHEN, H., ZHANG, X., ZHANG, J., WANG, Q., Tuning the decarboxylation selectivity for deoxygenation of vegetable oil over Pt-Ni bimetal catalysts via surface engineering, *Catalysis Science & Technology*, 8(4), 2018, 1126-1133.
32.AKYALCIN, S., Kinetic study of the hydration of propylene oxide in the presence of heterogeneous catalyst. Chem. Ind. Chem. Eng. Q. 2017;23(4):573−580.
33.VLACHOS, N., SKOPELITIS, Y., PSAROUDAKI, M., KONSTANTINIDOU, V., CHATZILAZAROU, A., TEGOU, E., Applications of Fourier transform-infrared spectroscopy to edible oils, *Analytica Chimica Acta*, 573-574, 2006, 459-465.
34.OSMONT, A., YAHYAOUI, M., CATOIRE, L., GÖKALP, I., SWIHART, M.T., Thermochemistry of CO, (CO)O, and (CO)C bond breaking in fatty acid methyl esters, *Combustion and Flame*, 155(1), 2008, 334-342.
35.OSMONT, A., CATOIRE, L., GÖKALP, I., SWIHART, M.T., Thermochemistry of C−C and C−H Bond Breaking in Fatty Acid Methyl Esters, *Energy & Fuels*, 21(4), 2007, 2027-2032.
36.LI, D., XIN, H., DU, X., HAO, X., LIU, Q., HU, C., Recent advances for the production of hydrocarbon biofuel via deoxygenation progress, *Science Bulletin*, 60(24), 2015, 2096-2106.

Manuscript received: 18.04.2020